

Editor's Choice

Chlorogenic Acid Protects DNA against Double-strand Breaks: Evidence from Single Molecule Observation

Haruto Ogawa,¹ Takashi Nishio,^{1,2} Yuko Yoshikawa,¹ Koichiro Sadakane,¹ and Kenichi Yoshikawa*^{1,3}¹Faculty of Life and Medical Sciences, Doshisha University, Kyoto 610-0394, Japan²Cluster of Excellence Physics of Life, TU Dresden, 01307 Dresden, Germany³Center for Integrative Medicine and Physics, Institute for Advanced Study, Kyoto University, Kyoto 606-8501, Japan

E-mail: keyoshik@mail.doshisha.ac.jp



K. Yoshikawa



H. Ogawa



T. Nishio



Y. Yoshikawa



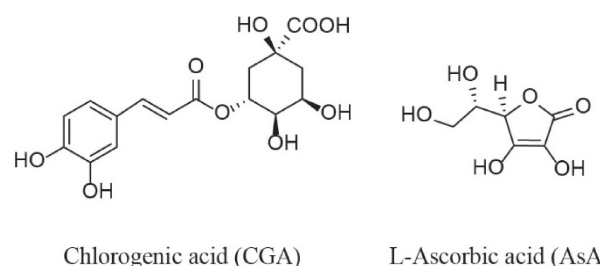
K. Sadakane

A natural polyphenol chlorogenic acid (CGA) is regarded as an antioxidant by preventing oxidative damage. Among the oxidative damages, DNA double-strand breaks (DSBs) are considered the most severe. To study the protective effect of CGA against DSBs, we measured the time-dependent increase of DSBs caused by photo-irradiation through a single molecule observation of DNA (166 kbp) using fluorescence microscopy. The results have been analyzed in relation to the two-step mechanism with single-strand breaks.

Keywords: Single-DNA observation | DNA double-strand breaks | Antioxidant chlorogenic acid

Polyphenols found in many plants and foods have favorable biological effects (e.g., antioxidant and anti-inflammatory activities) on human health.^{1–7} A major beneficial effect of polyphenols is to prevent oxidative damage in living cells by suppressing the production of reactive oxygen species (ROS). High ROS levels lead to protein modifications, lipid peroxidation-mediated membrane damage, and DNA damage.^{8–12} Among DNA damage, double-strand breaks (DSBs) are the most toxic in the cell and can result in genome instability, leading to cancer and cell death.^{13–20} Recently, the use of polyphenols as chemopreventive agents to protect against oxidative stress and DNA damage in photo-exposed skin is gaining greater attention.^{20–23} Chlorogenic acid, ((1S,3R,4R,5R)-3-[[[(E)-3-(3,4-dihydroxyphenyl)prop-2-enoyl]-oxy]-1,4,5-trihydroxy-cyclohexane-1-carboxylic acid, CGA) (Scheme 1), is one of the most available polyphenols found in various foods such as fruits, vegetables, wine, olive oil, coffee, and tea.^{4,5,24–28} The amount of CGA contained in a cup of coffee is 200–400 μmol/100 mL.^{4,5,29,30} Several studies have reported the antioxidant effect of CGA in relation to the possible beneficial effects of coffee, including anti-aging effects and protective effects against neuronal diseases like Alzheimer's and Parkinson's.^{31–35}

As for the measurements of DSBs in DNA molecules, numerous studies have been performed through methodologies such as immunological assays and the comet assay. Unfortunately, it is difficult to reliably estimate the number of DSBs with these methodologies, especially for genome-size long DNA molecules. Recently, the direct visualization of a single giant DNA molecule using fluorescence microscopy has provided useful information on the structure and function of genome-size



Scheme 1. Chemical structures of chlorogenic acid (CGA) and L-ascorbic acid (AsA).

DNA molecules,^{36–45} including the application to analyze DSBs in a measurable manner. In the present study, we quantified the protective effect of CGA against ROS by calculating the amount of DSBs generated in a genome-size DNA molecule using a single molecular observation technique and compared its protective effect with L-ascorbic acid, AsA, (Scheme 1). We utilized the fluorescence dye YOYO-1, (quinolinium, 1,1'-[1,3-propanediylbis[(dimethyliminio)-3,1-propanediyl]]bis[4-[(3-methyl-2(3H)-benzoxazolylidene)methyl]]-tetraiodide), to visualize individual DNA molecules under fluorescence microscopy.^{31,32,34,37–39,42}

It is well known that YOYO-1 generates ROS, including hydroxyl radicals, under photo-irradiation. We thus adapted YOYO-1 to induce ROS and observe single DNA molecules.^{36,37,39–41,45} T4 GT7 DNA (166 kbp, contour length 57 μm) was purchased from Nippon Gene (Tokyo, Japan). The fluorescent cyanine dye, YOYO-1, was purchased from Molecular Probes, Inc. (Oregon, USA). Antioxidants, 2-mercaptoethanol (2-ME) and L-ascorbic acid (AsA), were purchased from Wako Pure Chemical Industries (Osaka, Japan). CGA was purchased from Cayman Chemical, Inc. (Michigan, USA) (Scheme 1).

T4 GT7 DNA (0.3 μM in nucleotide units) was dissolved in 10 mM Tris-HCl (pH 7.4) with YOYO-1 (0.05 μM). On the measurements for individual DNA molecules fluctuating in solution, YOYO-1 was used as a fluorescence dye to visualize DNA molecules and also adapted as a photosensitizer to generate ROS,^{36,37,39–41,45} where focused UV-light irradiation (450–490 nm) was used. Measurements were conducted using a low DNA concentration to avoid intermolecular DNA aggregation. Fluorescence images of DNA molecules were observed using the Axio Observer A1 inverted fluorescence microscope (Zeiss,

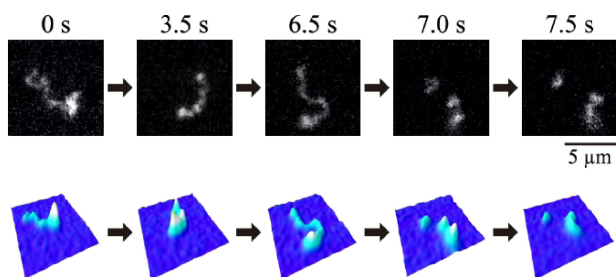


Figure 1. Representative images of the real-time formation of double-strand breaks (DSBs) caused by photo-irradiation-induced reactive oxygen species (ROS). Fluorescence microscopic images of a single T4 GT7 DNA molecule under photo-irradiation (upper panel), and the corresponding quasi-three-dimensional profiles of the fluorescence intensity distribution (bottom panel). YOYO-1 (0.05 μM) was used as the fluorescence dye and photosensitizer. The solution did not contain CGA or AsA.

Oberkochen, Germany), equipped with a 100x objective lens. 2-ME (4%; v/v) was added to all of the samples prior to fluorescence imaging to slow the photo-breakage reaction to a level suitable for real-time observations. Images were obtained with a digital CMOS camera (Hamamatsu Photonics, Hamamatsu, Japan). The recorded video images were analyzed with ImageJ (National Institute of Mental Health, MD, USA). All observations were carried out at room temperature (24 °C).

DSBs of a single T4 GT7 DNA molecule were observed at an individual DNA molecule level and in real time (Figure 1). YOYO-1 was adapted as a photosensitizer to generate ROS and used as a fluorescence dye to visualize individual DNA molecules fluctuating in solution. The corresponding quasi-three-dimensional images represent the fluorescence intensity distribution for a DNA molecule (Figure 1, bottom panel). The breaking time, t , was evaluated for the period from the start of the focused photo-illumination until the occurrence of the first DSB.

Figure 2a shows the time-course for the increase of photo-irradiation-induced DSBs in solutions with different concentrations of CGA, together with the data of AsA (1 μM and 10 μM) for comparison. We performed the measurements for 50 DNA molecules at each condition. The vertical axis indicates the percentage of damaged DNA molecules (DSBs) and the horizontal axis, Breaking Time, shows the time from the moment of focusing of photo-irradiation on individual DNA molecules to the first DSB in solution. The amount of DNA molecules surviving without DSB increased with the increase of CGA concentration. The observed time-dependent profile is expected to reflect the underlying mechanism of DSBs formation; either a one-step reaction or a two-step reaction with single-strand breaks (SSBs).^{36,37,39–41,45}

The probability of surviving DNA, P , is shown in Figure 2b, graphed as a logarithm on the vertical axis versus the square of real-time, t^2 (horizontal axis). $P = 1 - [\text{probability of damaged DNA}]$. The linear correlation between the square of breaking time and $\ln(P)$ in Figure 2b suggests that DSBs form as the product of two independent events (i.e., DSBs are induced via a two-step mechanism). This theoretical hypothesis of DSB formation kinetics has been proposed in our past studies.^{36,37,39–41,45} We briefly discuss this issue here. In the case of SSBs caused by

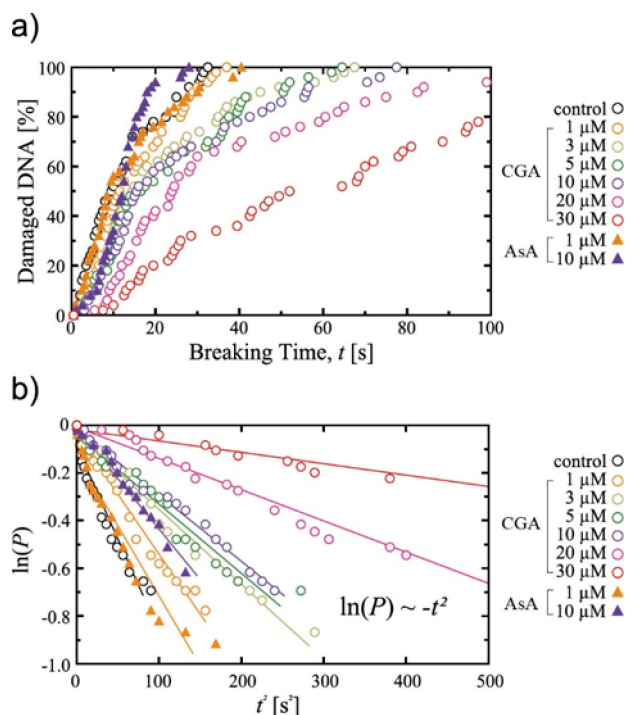


Figure 2. Photo-induced DSBs. (a) Time-dependence of the percentage of damaged DNA molecules at different CGA concentrations and AsA (1 μM and 10 μM). The breaking time, t , was evaluated for the period from the start of the focused photo-irradiation on individual DNA molecules until the occurrence of the first DSB. (b) The relationship between the horizontal axis, t^2 , and the vertical axis, $\ln(P)$, where P is the probability of surviving DNA molecules, which was calculated as $P = 1 - [\text{probability of damaged DNA}]$. As in eq (3), the kinetic constants, A [s⁻²], are obtained from the slopes in Figure 2b.

ROS, nicks are randomly generated along double-stranded DNA molecules under irradiation, and fragmentation of a DNA molecule (i.e., DSB) is produced by an additional SSB near an existing SSB.

Under stationary photo-illumination with a power I , the number of nicks along a single DNA molecule will increase as shown in eq (1), where α is a positive constant:

$$\frac{dn}{dt} = \alpha I \quad (1)$$

By adapting the assumption that the decrease in P can be represented as the product of n and P , time-dependence of P is given as constant,

$$\frac{dP}{dt} = -\beta nP = \alpha\beta ItP \quad (2)$$

where β is the rate constant for the generation of a DSB from a nick along a DNA chain. We adapted the initial condition that $n = 0$ and $P = 1$ at $t = 0$. Thus, we obtain:

$$\ln(P) = -At^2 \quad (3)$$

where $A (= (1/2)\alpha\beta I)$ is the rescaled kinetic constant. The linear relationship between the square of the time and $\ln(P)$ in Figure 2b confirms the above-mentioned two-step reactions.

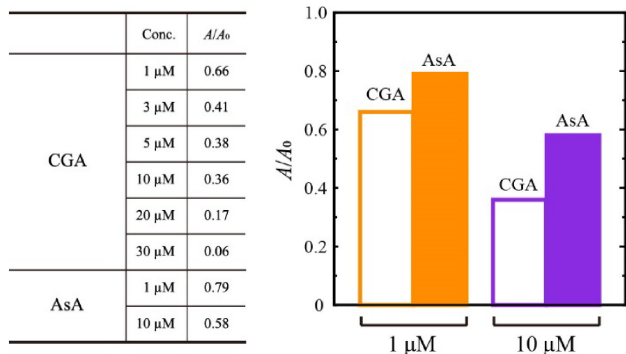


Figure 3. Relative kinetic constant, A/A_0 , for the generation of DSBs, where A_0 corresponds to the control experiment. Left panel: The values of A/A_0 obtained from the slopes of Figure 2b at different concentrations of CGA and AsA. The experimental errors are estimated as 20–30%. Right graph: Comparison of A/A_0 between CGA and AsA at 1 and 10 μ M.

The protective effects of CGA increased with an escalation in the CGA concentration (Figure 2a). The relative kinetic constants of DSBs formation, A/A_0 , were determined from the graph slopes in Figure 2b, where A_0 is the constant in the absence of antioxidative chemicals.

These relative kinetic constants are summarized in Figure 3. CGA reduced the rate of DNA DSBs to about 66% at 1 μ M and 6% at 30 μ M. Interestingly, CGA decreased A/A_0 values by 0.34 and 0.64 at 1 μ M and 10 μ M, respectively, from the control. On the other hand, the decrease by AsA was 0.21 and 0.42, respectively. These results indicate that CGA has ca. 1.5–1.6 times greater antioxidative potency than AsA.

The protective activity against DSB formation was dependent on the concentration of CGA used. In our experimental system, we adapted continuous photo-irradiation to generate ROS. The rate of nick-formation, or SSBs, corresponded to the kinetics of eq (1), and should be proportional to the concentration of ROS [ROS]. We assumed the rate of the second step for DSB formation, eq (2), would also be proportional to [ROS]. Under such approximations, the kinetic constant for the formation of DSBs is regarded to be proportional to the square of [ROS] as a simple estimate, by denoting the concentration of ROS under the constant strength of photo-irradiation to be [ROS] $_0$.

$$\frac{A}{A_0} \sim \frac{[ROS]^2}{[ROS]_0^2} \quad (4)$$

Antioxidants, such as CGA and AsA, are generally considered to decrease the amount of ROS as a mean to prevent the formation of DSBs. Under the simple assumption that the decrease of ROS is expressed as the multiplication product of [ROS] $_0$ and [CGA], the reduction of ROS caused by the antioxidant CGA would be given as

$$\Delta[ROS] = [ROS]_0 - [ROS] = \zeta [ROS]_0 [CGA] \quad (5)$$

where ζ is a constant corresponding to the efficiency of the redox reaction. This relationship is transformed as

$$1 - \frac{[ROS]}{[ROS]_0} = \zeta [CGA] \quad (6)$$

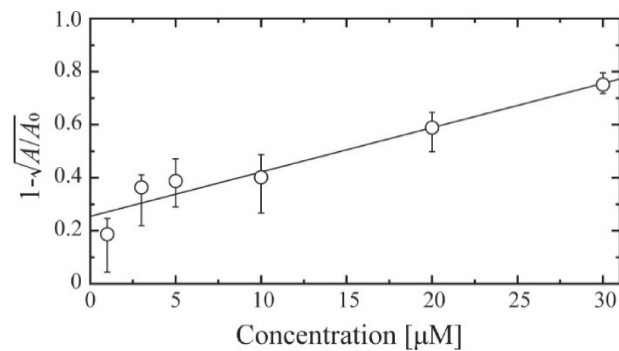


Figure 4. Relationship between CGA concentration and $1 - \sqrt{A/A_0}$ (see eq (7)). ($1 - \sqrt{A/A_0}$) corresponding to the protection/decrease of the probability of single-strand break (SSB).

By replacing the second term in the left-hand side of eq (4), we obtain the following relationship,

$$1 - \sqrt{\frac{A}{A_0}} \approx \zeta [CGA] \quad (7)$$

ROS randomly cause SSBs, and DSBs results when SSBs occur on opposite sides of double-strand DNA. We expect the rate constant for the formation of DSBs to be proportional to the product of the rate constant for the formation of SSBs. Therefore, we graphed the protective effect for SSB, ($1 - \sqrt{A/A_0}$), on the vertical axis and concentration of CGA on the horizontal axis (Figure 4). The linear relationship in the figure supports the working hypothesis that DSBs are induced through a two-step occurrence of SSBs caused by ROS. The analyses of Figure 2b and Figure 4 both justify the kinetics of successive SSBs being the fundamental mechanism of DSBs formation.

The protective effects of CGA against DSBs formed in a genome-size DNA molecule (166 kbp) were quantitated by the application of single molecule observation with fluorescence microscopy. The fluorescent dye, YOYO-1, was adapted to visualize individual DNA molecules and to generate ROS under constant photo-irradiation. CGA protected against the formation of DSBs, observed over time and as low as 1 μ M. CGA exhibited a greater protective effect than AsA at the same concentration (1 μ M and 10 μ M). The formation of DSBs was time-dependent and observed as a linear relationship of $\ln(P) \sim -t^2$, where P is the surviving probability of intact DNA against DSBs and t is the time under irradiation. This relationship suggests that DSBs are caused by a two-step SSB mechanism. Further analysis validated our proposed underlying mechanism of DSB generation on DNA, caused by photo-induced ROS, based on the kinetic constants of DSB formation with different concentrations of CGA. Numerous studies have reported that CGA exhibits antioxidant activity at concentrations of several hundred μ M or mM by using UV-Vis spectroscopic observations of reactive chemical species (e.g., DPPH (1,1-diphenyl-2-picryl-hydrazyl) and DMPD (*N,N*-dimethyl-*p*-phenylenediamine)).^{46–49} In the present study, we have evaluated the protective effect of CGA against DSBs in genome-size DNA. It is highly expected that further application of single-DNA observation will be used to evaluate the probability and kinetics of DSB formation in the presence of various kinds of antioxidants and oxidants among biological and synthetic chemicals.

This work was partially supported by JSPS KAKENHI Grants (JP20H01877 to K.Y., and JP22K20640 and JP23K14159 to T.N.), by JST SPRING (JPMJSP2129 to T.N.), and by grants from the Uehara Memorial Foundation (to T.N.). T.N. was supported by the Deutsche Forschungsgemeinschaft (DFG, German Research Foundation) under Germany's Excellence Strategy—EXC 2068—390729961—Cluster of Excellence Physics of Life of TU Dresden.

References

- 1 A. Scalbert, I. T. Johnson, M. Saltmarsh, *Am. J. Clin. Nutr.* **2005**, *81*, 215S.
- 2 B. Halliwell, *Cardiovasc. Res.* **2007**, *73*, 341.
- 3 R. Tsao, *Nutrients* **2010**, *2*, 1231.
- 4 S. F. Nabavi, S. Tejada, W. N. Setzer, O. Gortzi, A. Sureda, N. Braidy, M. Daglia, A. Manayi, S. M. Nabavi, *Curr. Neuropharmacol.* **2017**, *15*, 471.
- 5 C. G. Fraga, K. D. Croft, D. O. Kennedy, F. A. Tomás-Barberán, *Food Funct.* **2019**, *10*, 514.
- 6 Z. Yan, Y. Zhong, Y. Duan, Q. Chen, F. Li, *Anim. Nutr.* **2020**, *6*, 115.
- 7 A. Rana, M. Samtiya, T. Dhewa, V. Mishra, R. E. Aluko, *J. Food Biochem.* **2022**, *46*, e14264.
- 8 B. Halliwell, O. I. Aruoma, *FEBS Lett.* **1991**, *281*, 9.
- 9 J. E. Park, J.-H. Yang, S. J. Yoon, J.-H. Lee, E. S. Yang, J.-W. Park, *Biochimie* **2002**, *84*, 1198.
- 10 G. Stark, *J. Membr. Biol.* **2005**, *205*, 1.
- 11 C. A. Juan, J. M. P. de la Lastra, F. J. Plou, E. Pérez-Lebeña, *Int. J. Mol. Sci.* **2021**, *22*, 4642.
- 12 M. I. Anik, N. Mahmud, A. A. Masud, M. I. Khan, M. N. Islam, S. Uddin, M. K. Hossain, *ACS Appl. Bio Mater.* **2022**, *5*, 4028.
- 13 M. Fenech, *Ann. N.Y. Acad. Sci.* **1998**, *854*, 23.
- 14 W. F. Morgan, J. Corcoran, A. Hartmann, M. I. Kaplan, C. L. Limoli, B. Ponnaiya, *Mutat. Res.* **1998**, *404*, 125.
- 15 P. L. Olive, *Radiat. Res.* **1998**, *150*, S42.
- 16 W. P. Roos, B. Kaina, *Trends Mol. Med.* **2006**, *12*, 440.
- 17 A. F. Swindall, J. A. Stanley, E. S. Yang, *Cancers (Basel)* **2013**, *5*, 943.
- 18 M. E. Lomax, L. K. Folkes, P. O'Neill, *Clin. Oncol.* **2013**, *25*, 578.
- 19 U. S. Srinivas, B. W. Q. Tan, B. A. Vellayappan, A. D. Jeyasekharan, *Redox Biol.* **2019**, *25*, 101084.
- 20 F. Tamanoi, K. Yoshiakawa, Elsevier, The Netherlands, **2022**, *The Enzymes* Vol. 51, pp. 2–152.
- 21 S. Saric, R. K. Sivamani, *Int. J. Mol. Sci.* **2016**, *17*, 1521.
- 22 V. Kostyuk, A. Potapovich, A. R. Albuhaydar, W. Mayer, C. De Luca, L. Korkina, *Rejuvenation Res.* **2018**, *21*, 91.
- 23 V. Jesumani, H. Du, P. Pei, M. Aslam, N. Huang, *PLoS One* **2020**, *15*, e0227308.
- 24 M. Richelle, I. Tavazzi, E. Offord, *J. Agric. Food Chem.* **2001**, *49*, 3438.
- 25 E. Anklam, *Anal. Bioanal. Chem.* **2005**, *382*, 10.
- 26 H. M. Rawel, S. E. Kulling, *J. Verbr. Lebensm.* **2007**, *2*, 399.
- 27 A. Yashin, Y. Yashin, J. Y. Wang, B. Nemzer, *Antioxidants* **2013**, *2*, 230.
- 28 N. Liang, D. D. Kitts, *Nutrients* **2016**, *8*, 16.
- 29 A. Stalmach, W. Mullen, D. Barron, K. Uchida, T. Yokota, C. Cavin, H. Steiling, G. Williamson, A. Crozier, *Drug Metab. Dispos.* **2009**, *37*, 1749.
- 30 A. Stalmach, G. Williamson, A. Crozier, *Food Funct.* **2014**, *5*, 1727.
- 31 O. Weinreb, S. Mandel, T. Amit, M. B. H. Youdim, *J. Nutr. Biochem.* **2004**, *15*, 506.
- 32 L. Rossi, S. Mazzitelli, M. Arciello, C. R. Capo, G. Rotilio, *Neurochem. Res.* **2008**, *33*, 2390.
- 33 N. Tajik, M. Tajik, I. Mack, P. Enck, *Eur. J. Nutr.* **2017**, *56*, 2215.
- 34 H. Cory, S. Passarelli, J. Szeto, M. Tamez, J. Mattei, *Front. Nutr.* **2018**, *5*, Article 87.
- 35 A. Farah, J. de Paula Lima, *Beverages* **2019**, *5*, 11.
- 36 Y. Yoshikawa, M. Suzuki, N. Yamada, K. Yoshikawa, *FEBS Lett.* **2004**, *566*, 39.
- 37 Y. Yoshikawa, T. Mori, M. Suzuki, T. Imanaka, K. Yoshikawa, *Chem. Phys. Lett.* **2010**, *501*, 146.
- 38 A. Estévez-Torres, D. Baigl, *Soft Matter* **2011**, *7*, 6746.
- 39 K. Yoshida, N. Ogawa, Y. Kagawa, H. Tabata, Y. Watanabe, T. Kenmotsu, Y. Yoshikawa, K. Yoshikawa, *Appl. Phys. Lett.* **2013**, *103*, 063705.
- 40 Y. Ma, N. Ogawa, Y. Yoshikawa, T. Mori, T. Imanaka, Y. Watanabe, K. Yoshikawa, *Chem. Phys. Lett.* **2015**, *638*, 205.
- 41 M. Noda, Y. Ma, Y. Yoshikawa, T. Imanaka, T. Mori, M. Furuta, T. Tsuruyama, K. Yoshikawa, *Sci. Rep.* **2017**, *7*, 8557.
- 42 A. Zinchenko, N. V. Berezhnoy, S. Wang, W. N. Rosencrans, N. Korolev, J. R. C. van der Maarel, L. Nordenskiöld, *Nucleic Acids Res.* **2018**, *46*, 635.
- 43 T. Nishio, Y. Yoshikawa, K. Yoshikawa, S. Sato, *Sci. Rep.* **2021**, *11*, 11739.
- 44 K. Fujino, T. Nishio, K. Fujioka, Y. Yoshikawa, T. Kenmotsu, K. Yoshikawa, *Polymers* **2023**, *15*, 149.
- 45 K. Yoshikawa, *Enzymes* **2022**, *51*, 7.
- 46 M. Terashima, I. Nakatani, A. Harima, S. Nakamura, M. Shiiba, *J. Agric. Food Chem.* **2007**, *55*, 165.
- 47 J. P. Adjimani, P. Asare, *Toxicol. Rep.* **2015**, *2*, 721.
- 48 A. Czyzowska, E. Klewicka, E. Pogorzelski, A. Nowak, *J. Food Compos. Anal.* **2015**, *39*, 62.
- 49 H. J. Jabeen, S. Saleemi, H. Razzaq, A. Yaqub, S. Shakoore, R. Qureshi, *J. Photochem. Photobiol., B* **2018**, *180*, 268.